

Dipolar Dark Matter

Eduard Massó¹, Subhendra Mohanty² and Soumya Rao²

¹*Grup de Física Teòrica and Institut de Física d'Altes Energies
Universitat Autònoma de Barcelona, 08193 Bellaterra, Spain*

²*Physical Research Laboratory, Ahmedabad 380009, India*

Abstract

If dark matter (DM) has non-zero direct or transition, electric or magnetic dipole moment then it can scatter nucleons electromagnetically in direct detection experiments. Using the results from experiments like XENON, CDMS, DAMA and CO-GENT we put bounds on the electric and magnetic dipole moments of DM. If DM consists of Dirac fermions with direct dipole moments, then DM of mass less than 10 GeV is consistent with the DAMA signal and with null results of other experiments. If on the other hand DM consists of Majorana fermions then they can have only non-zero transition moments between different mass eigenstates. We find that Majorana fermions with mass $m_\chi > 38$ GeV and mass splitting of the order of (50-200) keV can explain the DAMA signal and the null observations from other experiments and in addition give the observed relic density of DM by dipole-mediated annihilation. This parameter space for the mass and for dipole moments is allowed by limits from L3 but may have observable signals at LHC.

1 Introduction

Experimental observations mainly of dynamics of spiral galaxies and galaxy clusters indicate the existence of dark matter (DM). Cosmological observations confirm the existence of DM and in addition show that the bulk of it must be non-baryonic [1]. In this paper we consider weakly interacting massive particles (WIMPs) as candidates for DM, but we adopt a model independent and phenomenological approach.

The mass and cross section of the DM (which is expected to have a local density of about 0.3 GeV/cm^3 and velocity w.r.t the Earth of about 200 km/sec [2]) is probed by direct detection experiments like XENON [3], CDMS [4], DAMA [5] and COGENT [6]. These experiments detect DM scattering off nuclei by measuring the recoil energy of the nuclei. The energy threshold of such detectors is typically of the order of a few keV. Of these experiments, the DAMA experiment observed an annual modulation in its signal which could have been due to DM scattering. However none of the other experiments conducting direct DM searches have seen evidence of such an event. Theoretically if one considers spin-independent interaction [7, 8] of these WIMPs with the nuclei then it is found that only in the low mass range from about 5 to 10 GeV one can reconcile DAMA signal with the null results from other experiments. There have been proposals of inelastic scattering of DM [9] by nuclei which results in heavier DM mass being allowed for explaining all the existing data.

Although DM has zero electric charge it may couple to photons through loops in the form of electric and magnetic dipole moments. Here we study WIMPs which are endowed with such dipole moments and thus can interact feebly via electromagnetic interaction [10, 11].

We first will consider the case that DM is a Dirac fermion. The effective Lagrangian for coupling of a Dirac fermion χ having an electric dipole moment \mathcal{D} and a magnetic dipole moment μ to a electromagnetic field $\mathcal{F}^{\mu\nu}$ is

$$\mathcal{L}_{elast} = -\frac{i}{2} \bar{\chi} \sigma_{\mu\nu} (\mu + \gamma_5 \mathcal{D}) \chi \mathcal{F}^{\mu\nu}. \quad (1)$$

In this case, we have elastic scattering of DM by nuclei through a photon exchange (Fig.1). This is studied in detail for the case of electric dipole moment in Section 2 and of magnetic dipole moment in Section 4.

Next we consider the case of DM being Majorana fermions. These have only non-zero transition moments between different mass eigenstates. Their interaction with photons is described by

$$\mathcal{L}_{inel} = -\frac{i}{2} \bar{\chi}_2 \sigma_{\mu\nu} (\mu_{12} + \gamma_5 \mathcal{D}_{12}) \chi_1 \mathcal{F}^{\mu\nu} \quad (2)$$

where μ_{12} is the transition magnetic moment and \mathcal{D}_{12} is the transition electric moment. Majorana DM would have inelastic scattering off nuclei through a photon exchange. We study the case of transition electric dipole moment in Section 3 and of transition magnetic dipole moment in Section 4.

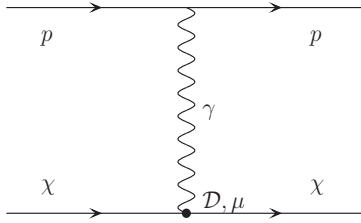


Figure 1: Electromagnetic scattering of a proton with DM with non-zero dipole moments.

In Section 5 we calculate the bounds on the dipole moments which would give the desired relic density abundance of DM.

In this paper we present two main types of results:

1. We find bounds on dipolar moments, direct and transition, coming from WIMP search experiments, which update the results in [11]. In addition we show that there are bounds on dipole moments from single photon search at LEP, an effect not discussed in [11].
2. We find regions in parameter space that are consistent with the positive signal from DAMA and with the null results from other experiments.

All these results are presented in Section 6. In Appendix A we give some details of our DM scattering calculations, and in Appendix B we show the DM annihilation cross section calculations which are relevant for the relic density results. In Appendix C we review the contact scalar interaction case, which is useful for comparison with our results.

2 Electric Dipole Moment Interaction of Dark Matter

The differential cross section for a DM-proton elastic scattering via interaction of the electric dipole moment of DM with the proton charge is given by

$$\frac{d\sigma}{dE_R} = \frac{e^2 \mathcal{D}^2}{4\pi v^2 E_R} \quad (3)$$

where \mathcal{D} is defined in (1). Here E_R is the recoil energy of proton and v is the speed of DM relative to the nucleus. The differential rate for nuclear scattering of DM through electric dipole moment interaction for a nucleus of Z protons and DM of mass m_χ is given by

$$\frac{dR}{dE_R} = Z^2 N_T \frac{\rho_\chi}{m_\chi} \int_{v>v_{min}} f(v) v \frac{d\sigma}{dE_R} dv \quad (4)$$

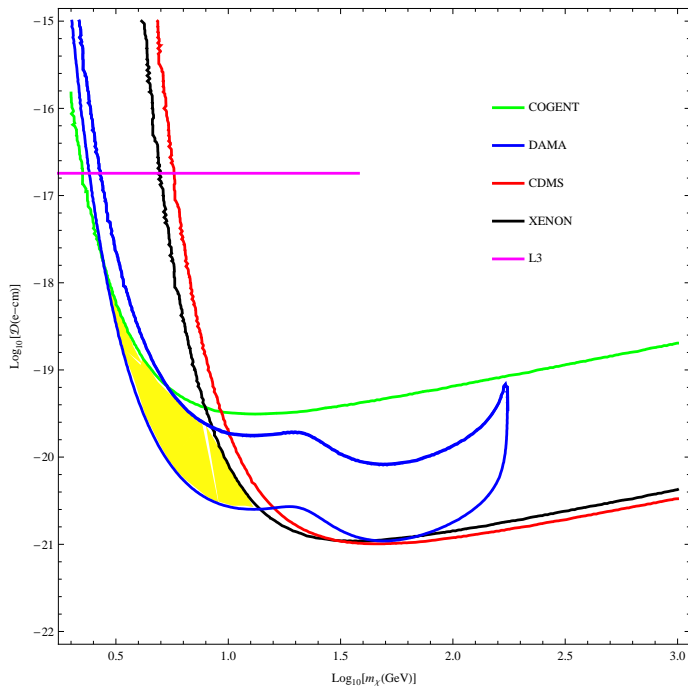


Figure 2: Plot shows the allowed regions for DM electric dipole moment with varying DM mass for elastic scattering for different experiments. Shaded region shows the allowed parameter space for DAMA which is consistent with all other experiments.

where N_T is the number of target nuclei in the detector and ρ_χ is the local DM density. The velocity distribution $f(v)$ and minimum speed of DM v_{min} , for a given energy threshold E_{Rmin} are given by [2]

$$f(v) = \frac{4v^2}{\sqrt{\pi}v_0^3} \exp\left(\frac{-v^2}{v_0^2}\right) \quad (5)$$

$$v_{min} = \sqrt{\frac{m_N E_{Rmin}}{2\mu_N^2}} \quad (6)$$

where m_N is the mass of the target nucleus, $\mu_N = m_\chi m_N / (m_\chi + m_N)$ is the reduced mass of the DM-nucleus system and $v_0 = 220$ km/sec. The factor Z^2 appearing in eqn.(4) shows the fact that this is a coherent scattering of the Z protons in the target nucleus. To determine the expected event rate R we integrate eqn.(4) over the nuclear recoil energy:

$$R = \int_{E_1/Q}^{E_2/Q} dE_R \epsilon(QE_R) \frac{dR}{dE_R}. \quad (7)$$

Here $\epsilon(QE_R)$ is the efficiency of the detector which depends on the recoil energy and Q is the quenching factor that relates the observed energy with the actual recoil energy

Experiment	Target nucleus	Quenching factor(Q)
DAMA	Na	0.3
	I	0.09
CDMS	Ge	1
XENON	Xe	1
COGENT	Ge	0.2

Table 1: Quenching factors for different experiments used in this analysis.

i.e $E_{Obs} = QE_R$. Q depends on the target nucleus and the nature of the detector. E_1 and E_2 are limits of the observed energy interval in a direct search experiment. Therefore E_1/Q and E_2/Q give the corresponding limits for the recoil energy E_R . Observed energies are usually quoted in units of electron equivalent energies (keVee). The detectors usually detect scintillation caused by electrons and thereby measure energy transferred to electrons by the nucleus. Q then represents the efficiency with which the recoil energy of nucleus is transferred to electrons which are detected by scintillation. The quenching factors for the different experiments analyzed here are given in Table 1.

In Fig.2 we show our results. The experiments give an upper limit which is a function of the DM mass m_χ , except for DAMA whose result is represented as an allowed band. We would like to point out that one can get a bound from the $e^+e^- \rightarrow \chi\chi\gamma$ process whose signal is a single photon detection with missing energy. From the analysis of the collaboration L3 [12] we get $\mathcal{D} < 6.6 \times 10^{-16}$ e-cm, valid for $m_\chi < 38$ GeV; this limit is also shown in Fig.2. We shall see the implications of this Figure in Section 6; there we shall also discuss the issue of the DM relic density.

3 Inelastic Dark Matter and Electric Dipole Moment Interaction

In this Section we consider the case that the WIMP is a Majorana particle, with a transition electric dipole moment \mathcal{D}_{12} as defined in (2). In this case we can have inelastic scattering $\chi_1 + N \rightarrow \chi_2 + N$ where χ_1 and χ_2 are two different mass eigenstates, and in general there is a mass difference between χ_1 and χ_2 , $\delta = m_2 - m_1$. Due to this mass difference, the minimum DM kinetic energy needed for the nucleon scattering becomes higher. DAMA has lower detection threshold compared to most experiments and therefore can be more sensitive to this scattering mode than the other experiments. This was first proposed in [9].

If we drop terms of higher order in δ (compared to m_χ) we end up with eqn.(3) for the

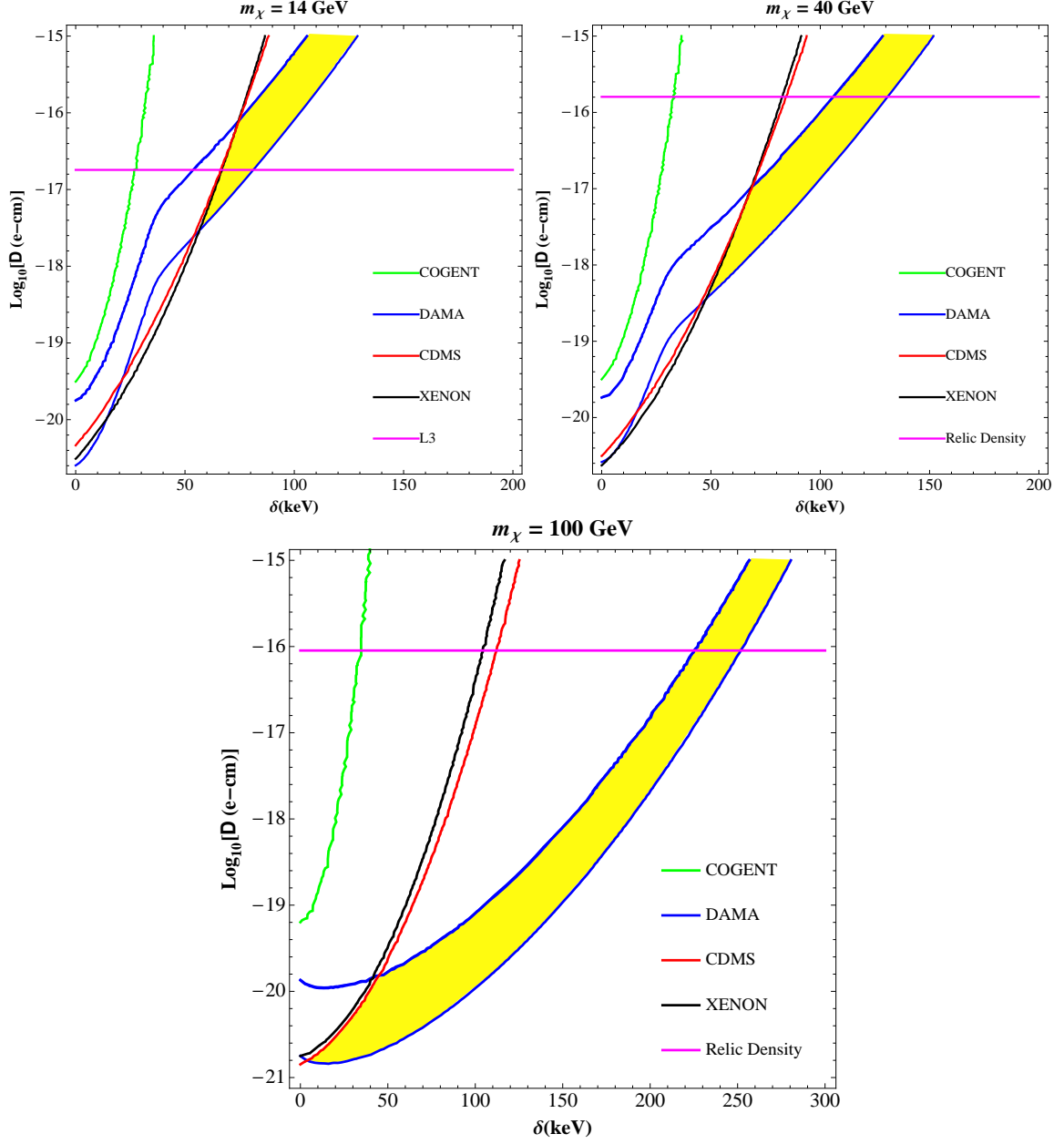


Figure 3: Plot of DM electric dipole moment against the mass difference δ for inelastic scattering for different experiments. Shaded region shows the allowed parameter space for DAMA which is consistent with all other experiments and in case of $m_\chi > 38 \text{ GeV}$ it is also consistent with the relic density.

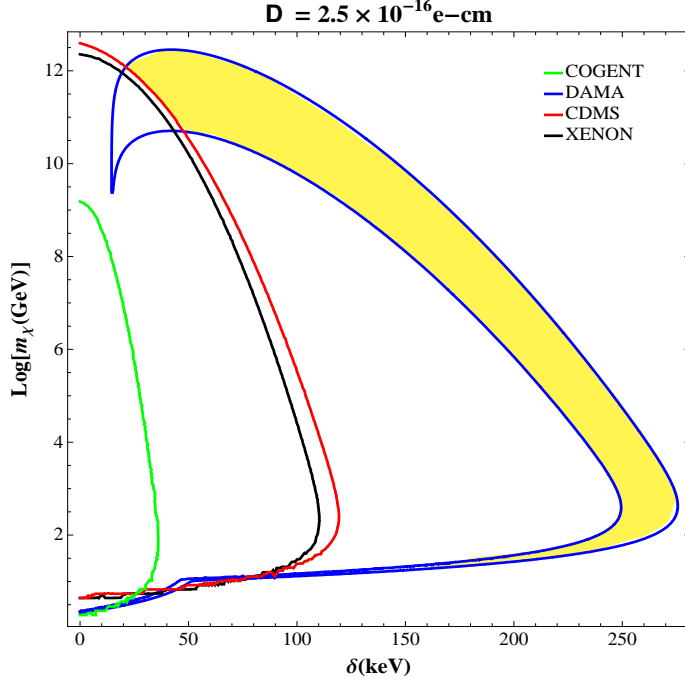


Figure 4: Plot of allowed DM mass and mass splitting δ for a fixed \mathcal{D} which gives the correct relic density of DM.

differential cross section. That is,

$$\frac{d\sigma_{inelastic}}{dE_R} = \frac{d\sigma_{elastic}}{dE_R}. \quad (8)$$

However the total cross section in the elastic and inelastic case are related to each other by a factor which enforces the condition of the minimum kinetic energy required for inelastic scattering. This relation has been derived at the end of Appendix A, and is given by,

$$\sigma_{inelastic} = \sqrt{1 - \frac{2\delta}{\mu_N v^2}} \sigma_{elastic}. \quad (9)$$

But we do not use the total cross section in our analysis, only the differential cross section and therefore the square root factor does not figure in our calculations. We integrate the differential cross section per unit recoil energy over the energy interval in which the experimental data have been observed. The only change from the analysis in the elastic case is that the minimum speed for scattering is now given by

$$v_{min} = \sqrt{\frac{1}{2m_N E_{Rmin}} \left(\frac{m_N E_{Rmin}}{\mu_N} + \delta \right)} \quad (10)$$

where notation has the same meaning as in the previous Section.

In Fig.3 we plot our results. We show a line for each direct search experiment and the allowed range is on the right of the line, except for DAMA that again is an allowed band. In the Figure we also plot the limit coming from LEP mentioned before, $\mathcal{D}_{12} < 6.6 \times 10^{-16}$ e-cm, which is the same than in the direct transition case if $|\delta| \ll m_\chi$. The collider limit applies provided $m_\chi < 38$ GeV.

Since in the inelastic case we have three parameters, namely, \mathcal{D}_{12} , m_χ , and δ , it is instructive to present Fig.4 where we fix \mathcal{D}_{12} and show the constraint in the (m_χ, δ) plane. Here the allowed regions is on the right of the curves of the different experiments except for DAMA which is again an allowed band.

We shall discuss the implications of all these limits in Section 6 and especially for the relic density in Section 5.

4 Magnetic Dipole Moment Interaction

The differential cross section per unit energy transfer for elastic scattering by a magnetic dipole moment interaction is given by

$$\frac{d\sigma}{dE_R} = \frac{e^2 \mu^2}{4\pi E_R} \left(1 + \frac{E_R}{2\mu_N v^2} \right). \quad (11)$$

In the case of inelastic scattering we get the same formula with μ substituted by the transition magnetic moment μ_{12} , provided we drop terms of higher order in the mass difference δ . Again, the only difference between elastic and inelastic is in the kinematics, because the minimum speed for inelastic scattering is given by eqn.(10). Fig.5 and Fig.6 show the results for magnetic dipole moment which are essentially the same as those for electric dipole moment in terms of the allowed parameter space from various experiments. In Fig.7 we plot the allowed regions in the space (m_χ, μ_{12}) .

In the next section we discuss the implications of dipolar DM vis a vis the DM relic density.

5 Relic Density of Dipolar DM

The relic abundance of dipolar DM is determined by the annihilation cross section $\chi\bar{\chi} \rightarrow f\bar{f}$ through a dipole vertex. In the case of Majorana fermions only non-identical fermions can annihilate ($\chi_1\bar{\chi}_2 \rightarrow f\bar{f}$) through the dipole channel as only the transition dipole moments $(\mathcal{D}_{12}, \mu_{12})$ are non-zero. When the mass difference δ between χ_1 and χ_2 is small the cross section for Majorana annihilation process is identical to that of the Dirac fermions (with \mathcal{D}, μ replaced with $\mathcal{D}_{12}, \mu_{12}$).

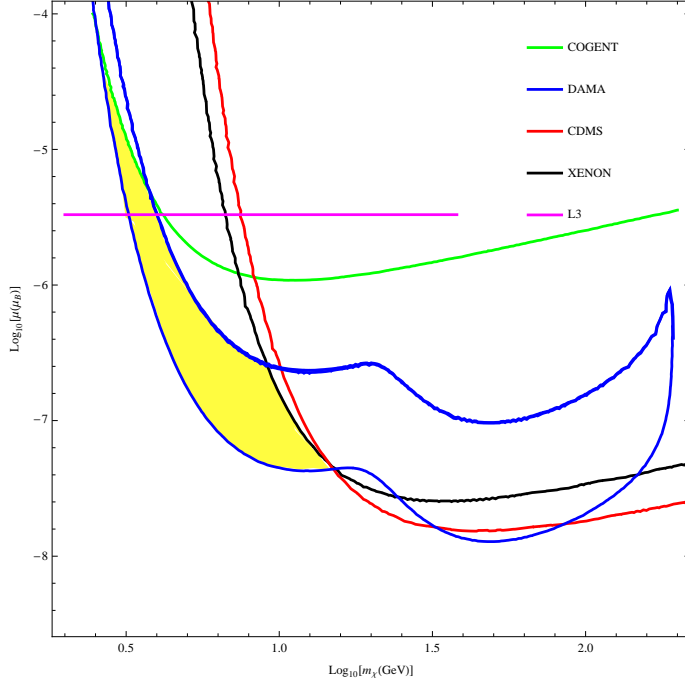


Figure 5: Plot shows the allowed regions for DM magnetic dipole moment with varying DM mass for elastic scattering for different experiments. Shaded region shows the allowed parameter space for DAMA which is consistent with all other experiments.

The annihilation cross section for electric dipole annihilation of DM for $\chi\bar{\chi} \rightarrow f\bar{f}$ is given by (see appendix B)

$$\sigma v_{rel} = \frac{e^2 \mathcal{D}^2}{48\pi} v_{rel}^2 \quad (12)$$

and the expression for the magnetic dipole annihilation case is

$$\begin{aligned} \sigma v_{rel} &= \frac{e^2 \mu^2}{4\pi} \left(1 - \frac{v_{rel}^2}{6}\right) \\ &\simeq \frac{e^2 \mu^2}{4\pi} \end{aligned} \quad (13)$$

where $v = 2\sqrt{1 - \frac{4m_\chi^2}{s}}$ is the relative velocity of the two annihilating WIMPs. The thermal averaged cross section, $\langle\sigma v_{rel}\rangle$, can be parameterized in terms of the temperature, $T = m_\chi \langle v^2 \rangle / 3$, where $v = v_{rel}/2$, such that

$$\langle\sigma v_{rel}\rangle \equiv \sigma_0 \left(\frac{T}{m_\chi}\right)^n \quad (14)$$

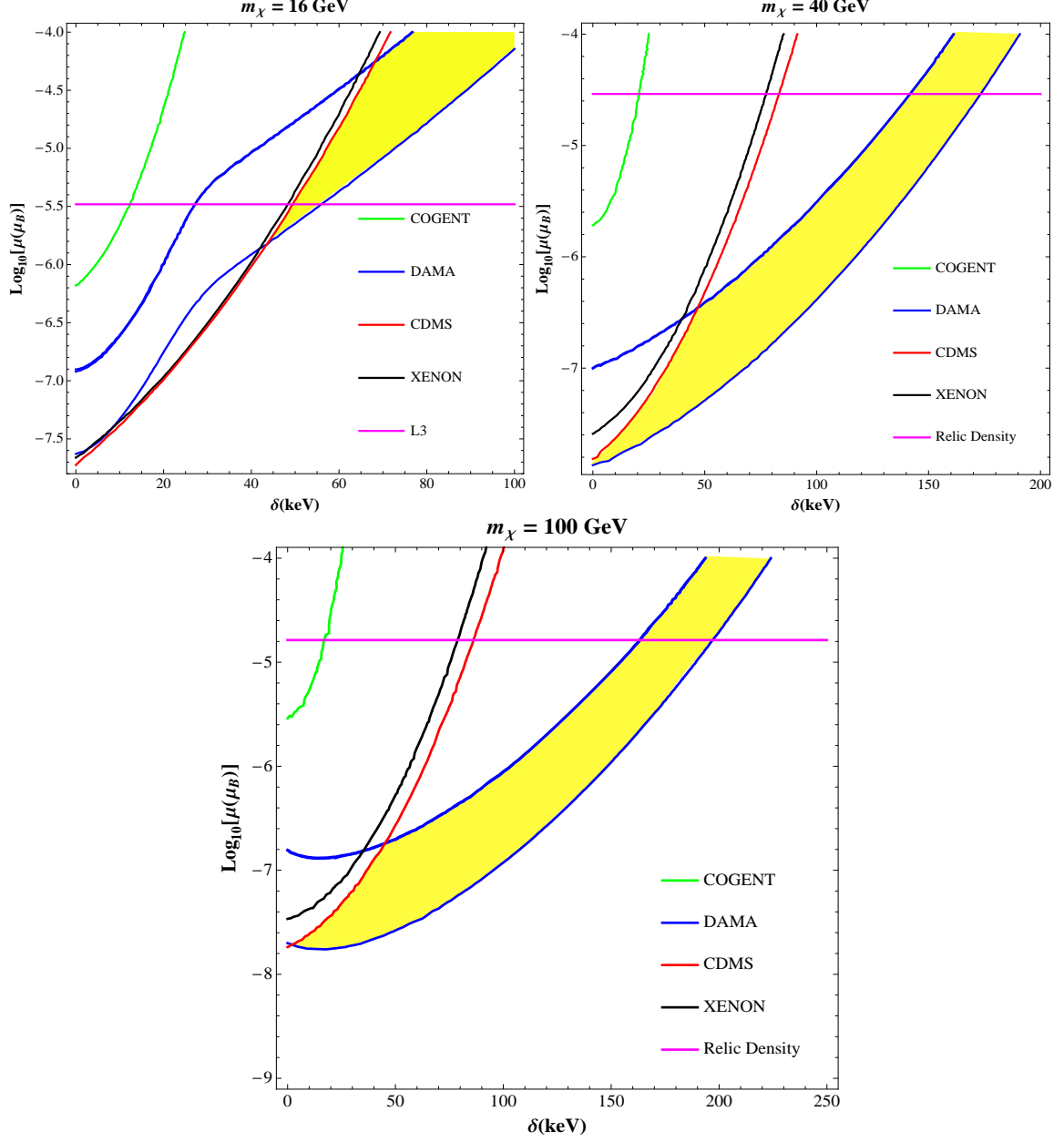


Figure 6: Plot of DM magnetic dipole moment against the mass difference δ for inelastic scattering for different experiments. Shaded region shows the allowed parameter space for DAMA which is consistent with all other experiments and in case of $m_\chi > 38 \text{ GeV}$ it is also consistent with the relic density.

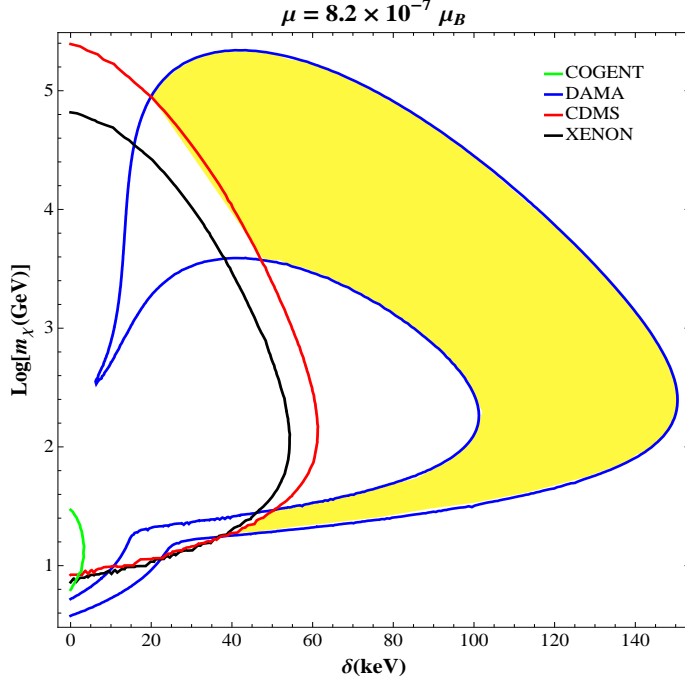


Figure 7: Plot of allowed DM mass and mass splitting δ for a fixed μ which gives the correct relic density of DM.

where n and the parameter σ_0 for magnetic and electric dipole interactions take the following values

$$\text{Magnetic Dipole: } \sigma_0 = \frac{e^2 \mu^2}{4\pi}, \quad n = 0 \quad (15)$$

$$\text{Electric Dipole: } \sigma_0 = \frac{3e^2 \mathcal{D}^2}{48\pi}, \quad n = 1 \quad (16)$$

Considering cold dark matter (CDM) we want to estimate the relic density in the context of dipolar interactions of such CDM candidates. The expression for $x_f = \frac{m_\chi}{T_f}$, where the subscript f indicates the freeze out condition, is given up to a reasonable approximation by [15]

$$x_f = \ln[0.038(n+1)(g/g_*^{1/2})m_{pl}m_\chi\sigma_0] - \left(n + \frac{1}{2}\right) \ln\{\ln[0.038(n+1)(g/g_*^{1/2})m_{pl}m_\chi\sigma_0]\} \quad (17)$$

where m_{pl} is Planck mass, while g and g_{*s} are the effective number of relativistic particles

at the time of decoupling. The DM relic density is then given by [15]

$$\Omega h^2 = 0.34 \left(\frac{(n+1)x_f^{n+1}}{(g_{*s}/g_*^{1/2})} \right) \frac{10^{-37} \text{cm}^2}{\sigma_0}. \quad (18)$$

The limit on cold dark matter density from WMAP [13] is $\Omega_m h^2 = 0.1099 \pm 0.0062$. Using (18), this gives us the bound on \mathcal{D} , which gives the acceptable relic density of dark matter, to be $\sim 2.5 \times 10^{-16}$ e-cm. For the magnetic dipole case again using (18) we find that the dipole moment must be $\sim 8.2 \times 10^{-7} \mu_B$.

For the case of non-identical Majorana annihilation the annihilation cross sections are identical to the case of Dirac fermions and the limits on the Dirac electric and magnetic moments from relic density abundance are identical to the bounds on transition magnetic moments given above.

6 Results and Conclusions

6.1 Direct dipole moments

We have explored the parameter space of electric and magnetic dipole moments of DM from the results of nuclear recoil experiments. We find that the limit on direct electric dipole moment is $\mathcal{D} < 1.6 \times 10^{-21}$ e-cm if the DM mass $m_\chi > 10$ GeV, see Fig.2. In this mass range there is no allowed parameter space which is consistent with the positive signal from DAMA and with the null results of other experiments.

For a DM mass $m_\chi = (3 - 13)$ GeV and a moment $\mathcal{D} \sim 2.5 \times 10^{-20}$ e-cm there is a region in parameter space where the DAMA signal is not ruled out by other experiments, see Fig.2.

For smaller masses, $m_\chi < 3$ GeV, the Figure shows that COGENT rules out DAMA. In Appendix C we review the scalar interaction mediated scattering (see Fig.8) where we see that DAMA is allowed by COGENT for any DM mass below about 15 GeV. This can be attributed to the fact that the DM interaction via electric dipole moment has a factor of recoil energy (E_R in the denominator of its cross section in eqn.(4)). This means that for low threshold this cross section is large and in the case of COGENT this threshold happens to be smaller than that for DAMA. But as the DM mass increases this advantage in favour of COGENT is nullified by the DM mass factor which again appears in the denominator of the cross section formulae.

The limit on direct magnetic dipole moment is $\mu < 10^{-8} \mu_B$ if the DM mass $m_\chi > 25$ GeV, see Fig.5. In this mass range there is no allowed parameter space which is consistent with a positive signal from DAMA with null results of other experiments. For DM masses $m_\chi = (3 - 12)$ GeV and $\mu \sim 6.3 \times 10^{-7} \mu_B$ there is a region in parameter space where the DAMA signal is not ruled out by other experiments, see Fig.5. Actually, in the low DM mass range the collider bound [12] is more restrictive than the direct WIMP search limits, as can be seen in Fig.5.

If the only interaction of DM with standard model particles had been via electromagnetic dipole interaction then the relic density of the DM particles would be determined uniquely from the annihilation cross section of the EM-dipole mediated process $\chi\chi \rightarrow f\bar{f}$ and m_χ . Such a calculation shows [11] that to get relic cold DM density consistent with WMAP measurement the dipole moments have to be in the range of $\mathcal{D} \simeq 5 \times 10^{-17}$ e-cm or $\mu \simeq 10^{-5}\mu_B$ when $m_\chi = (10 - 1000)$ GeV. The limits on DM dipole moments that we obtain on the basis of nuclear scattering experiments are much lower. This means that the DM particles must have some other more dominant interaction which decouples at a temperature $T_f \sim m_\chi/10$ to give the correct relic abundance while the dipole interactions decouple much earlier and have no bearing on the present DM density. These other dominant interactions however must not dominate over dipole interactions in nuclear scattering in order for our bounds on dipole moments to be meaningful. A good example of such a situation is seen in certain classes of WIMP models [2], where the interaction with standard model particles can be by Higgs exchange which gives rise to spin-independent (SI) interactions with nucleons or by Z exchange which gives rise to spin-dependent (SD) interactions [14]. When the nuclear scattering is by SD interaction then there is no coherent enhancement of the cross section by the atomic number. The bounds on the cross section for SI interactions is therefore more stringent than the bounds on SD interactions. The bounds for SI interactions from nuclear scattering experiments is $\sigma_{SI} < 5 \times 10^{-44}$ cm² and for SD interactions it is $\sigma_{SD} < 5 \times 10^{-28}$ cm² (for $m_\chi \sim 100$ GeV). Our bounds are relevant for WIMPs which can have a large spin-dependent cross section $\sigma_{SD} \simeq 0.3 \times 10^{-39}$ cm² to give the correct relic density, but this cross section is too small to be observed in nuclear scattering experiments.

6.2 Transition dipole moments

In Figs.3 and 6 we plot the constraints on the transition dipole moments \mathcal{D}_{12} and μ_{12} , respectively, versus the DM mass m_χ . We have fixed three values for the mass $m_\chi = 14, 40$ and 100 GeV, in order to illustrate our findings.

We see that a common feature of the plots is that the region where DAMA is consistent with other experiments is quite large and extends to higher and higher inelasticities. However for $m_\chi < 38$ GeV the region is further constrained by the collider bound from L3, and the allowed region is reduced. The allowed area is more and more reduced as we lower m_χ and for $m_\chi < 10$ GeV there is no region at all. For $m_\chi > 38$ GeV there is no collider bound and the region is large.

The most interesting aspect of the experimentally allowed parameter space for transition dipole moments is that the cosmologically preferred value (for getting the correct relic abundance) $\mathcal{D}_{ij} \sim 10^{-16}$ e-cm or $\mu_{ij} \sim 10^{-5}\mu_B$ [11] is consistent with the allowed values DAMA and other experiments when $m_\chi \gtrsim 38$ GeV and the mass split $\delta \simeq (50 - 100)$ keV. Thus, we find that transition dipole scattering has a large parameter space where the results of DAMA, the null results from other experiments and cosmological relic abundance are all consistent.

The event rates depend upon m_χ and \mathcal{D} or μ as \mathcal{D}^2/m_χ or μ^2/m_χ respectively. The dipole moments can increase by four orders of magnitude from the $\mathcal{D} = 10^{-20}$ e-cm to $\mathcal{D} = 10^{-16}$ e-cm (and similarly for the case of magnetic moments) and the same event rates would be obtained if mass is increased by eight orders of magnitude from 10^2 GeV to 10^{10} GeV. The range of DM mass for which DAMA is consistent with cosmology and L3 is therefore quite large, $38 \text{ GeV} < m_\chi < 10^{10} \text{ GeV}$. This parameter space of m_χ and electric /magnetic moments can give rise to a missing energy signal via the process $pp \rightarrow \chi_1 \chi_2 \gamma + \text{hadronic jets}$, and the dipolar model of dark matter may be testable at the LHC.

Acknowledgements

E.M. would like to thank Alessio Provenza for useful comments. E.M. acknowledges support by the CICYT Research Project FPA 2008-01430 and the Departament d'Universitats, Recerca i Societat de la Informació (DURSI), Project 2005SGR00916 and partly by the European Union through the Marie Curie Research and Training Network "UniverseNet" (MRTN-CT-2006-035863).

Appendix A: Cross Section Calculation for Electric and Magnetic Dipole Moment Interactions with Nuclei

Here we consider the elastic scattering process $\chi + p \rightarrow \chi + p$. We calculate the cross section in the lab frame where the proton is at rest initially. We assume that even after the scattering the proton remains at rest since the momentum transferred is very small in this process. The entire calculation is done in the non-relativistic limit.

Electric Dipole Moment

The initial momenta of DM and proton are denoted by k_i and p_i respectively, while the final momenta are denoted by k_f and p_f respectively. The amplitude squared for this process is given by

$$\begin{aligned} \overline{|\mathcal{M}|^2} &= -\frac{e^2 \mathcal{D}^2 q_\alpha q_\beta}{4q^4} \text{Tr}[(\not{k}_f + m_\chi) \sigma^{\mu\alpha} \gamma_5 (\not{k}_i + m_\chi) \gamma_5 \sigma^{\nu\beta}] \times \text{Tr}[(\not{p}_f + m_p) \gamma_\mu (\not{p}_i + m_p) \gamma_\nu] \\ &= \frac{e^2 \mathcal{D}^2}{4q^2} [64(q \cdot p_i)(k_i \cdot p_i) + 32m_\chi^2(q \cdot p_i) - 16(q \cdot p_i)^2 - 8q^2(q \cdot p_i) - 64(k_i \cdot p_i)^2] \end{aligned} \quad (\text{A1})$$

where q is the momentum transferred, while m_χ and m_p are masses of DM and proton respectively. In writing the above equation we have made use of $k_f = k_i - q$ and $p_f = p_i + q$.

Here, $(q \cdot p_i) = m_p E_R$ and $k_i \cdot p_i \approx m_\chi m_p$. Hence we can drop terms containing $(q \cdot p_i)$ and its higher orders, keeping just the last term in eqn.(A1). This gives us

$$\overline{|\mathcal{M}|^2} = -\frac{16e^2 \mathcal{D}^2}{q^2} (m_\chi m_p)^2. \quad (\text{A2})$$

Using $q^2 = E_R^2 - 2m_p E_R \approx -2m_p E_R$ we finally arrive at the following expression for the amplitude squared,

$$\overline{|\mathcal{M}|^2} = \frac{8e^2 \mathcal{D}^2}{E_R} m_\chi^2 m_p. \quad (\text{A3})$$

Now, the differential cross section is given by

$$\begin{aligned} d\sigma &= \frac{1}{2m_p 2E_1 v} \frac{d^3 p_f}{(2\pi)^3 E_p} \frac{d^3 k_f}{(2\pi)^3 E_2} (2\pi)^4 \delta^4(p_i + k_i - p_f - k_f) \overline{|\mathcal{M}|^2} \\ &= \frac{1}{64\pi^2 m_p E_1 v} \frac{d^3 k_f}{E_2 E_p} \delta(m_p + E_1 - E_p - E_2) \overline{|\mathcal{M}|^2} \\ &= \frac{1}{64\pi^2 m_p E_1 v} \frac{|\vec{k}_f|}{E_p} d\Omega \overline{|\mathcal{M}|^2} \end{aligned} \quad (\text{A4})$$

where E_1 and E_2 are energies of the initial and final DM states. Also the recoil energy can be written as follows:

$$E_R = \frac{|\vec{q}|^2}{2m_p} = \frac{|\vec{k}_i|^2 + |\vec{k}_f|^2 - 2|\vec{k}_i||\vec{k}_f|\cos\theta}{2m_p}$$

therefore,

$$dE_R = -\frac{|\vec{k}_i||\vec{k}_f|}{m_p} d(\cos\theta).$$

And we know that $d\Omega = -2\pi d(\cos\theta)$, so we can write

$$d\Omega = 2\pi \frac{m_p}{|\vec{k}_i||\vec{k}_f|} dE_R, \quad (\text{A5})$$

Using this in eqn.(A4) we get

$$\begin{aligned} \frac{d\sigma}{dE_R} &= \frac{1}{32\pi E_1 v} \frac{1}{E_p |\vec{k}_i|} \overline{|\mathcal{M}|^2} \\ &= \frac{1}{32\pi E_1^2 E_p v^2} \overline{|\mathcal{M}|^2}. \end{aligned} \quad (\text{A6})$$

We use the approximations, $E_1^2 \approx m_\chi^2$ and $E_p \approx m_p$, which gives us

$$\frac{d\sigma}{dE_R} = \frac{1}{32\pi m_\chi^2 m_p v^2} \overline{|\mathcal{M}|^2}. \quad (\text{A7})$$

Substituting for $\overline{|\mathcal{M}|^2}$ from eqn.(A3) we get

$$\frac{d\sigma}{dE_R} = \frac{e^2 \mathcal{D}^2}{4\pi E_R v^2} \quad (\text{A8})$$

which is same as eqn.(3).

Magnetic Dipole Moment

The trace in this case is same as in the case of EDM but without any γ_5 in it. The amplitude squared for this process is given by

$$\begin{aligned} \overline{|\mathcal{M}|^2} &= \frac{e^2 \mu^2 q_\alpha q_\beta}{4q^4} \text{Tr}[(\not{k}_f + m_\chi) \sigma^{\mu\alpha} (\not{k}_i + m_\chi) \sigma^{\nu\beta}] \times \text{Tr}[(\not{p}_f + m_p) \gamma_\mu (\not{p}_i + m_p) \gamma_\nu] \\ &= \frac{4e^2 \mu^2}{q^2} [4(q \cdot p_i)(k_i \cdot p_i) - 4(q \cdot p_i)m_\chi^2 - (q \cdot p_i)^2 - 4(k_i \cdot p_i)^2 + 4m_\chi^2 m_p^2] \\ &\quad - \frac{4e^2 \mu^2}{q^4} [4(q \cdot p_i)^2 m_\chi^2]. \end{aligned} \quad (\text{A9})$$

Here we drop terms which are higher order in $q \cdot p_i$ except the last term which is enhanced by a factor of q^2 in the denominator. Thus we get

$$\overline{|\mathcal{M}|^2} = \frac{16e^2 \mu^2}{q^2} \left[(q \cdot p_i)(k_i \cdot p_i) - (q \cdot p_i)m_\chi^2 - (k_i \cdot p_i)^2 + m_\chi^2 m_p^2 - \frac{(q \cdot p_i)^2 m_\chi^2}{q^2} \right] \quad (\text{A10})$$

where

$$\begin{aligned} q \cdot p_i &= m_p E_R \\ k_i \cdot p_i &\approx m_\chi m_p \\ (k_i \cdot p_i)^2 &\approx m_\chi^2 m_p^2 + m_\chi^2 m_p^2 v^2 \end{aligned}$$

Using these results in eqn.(A10) we get

$$\overline{|\mathcal{M}|^2} = \frac{16e^2 \mu^2}{q^2} \left[m_\chi m_p^2 E_R - m_p m_\chi^2 E_R - m_\chi^2 m_p^2 v^2 - \frac{m_\chi^2 m_p^2 E_R^2}{q^2} \right]. \quad (\text{A11})$$

Again using $q^2 \approx -2m_p E_R$ gives

$$\begin{aligned} \overline{|\mathcal{M}|^2} &= \frac{8e^2 \mu^2}{E_R} \left[m_\chi^2 m_p v^2 + m_\chi^2 E_R - m_\chi m_p E_R - \frac{m_\chi^2 E_R}{2} \right] \\ &= \frac{8e^2 \mu^2}{E_R} \left[m_\chi^2 m_p v^2 + \frac{m_\chi^2 E_R}{2} - m_\chi m_p E_R \right]. \end{aligned} \quad (\text{A12})$$

The differential cross section per unit recoil energy is given by eqn.(A7). Substituting from the above equation in eqn.(A7) we get

$$\begin{aligned}\frac{d\sigma}{dE_R} &= \frac{e^2\mu^2}{4\pi E_R} \left[1 + \frac{E_R}{2m_p v^2} - \frac{E_R}{m_\chi v^2} \right] \\ &= \frac{e^2\mu^2}{4\pi E_R} \left[1 + \frac{E_R}{2\mu_p v^2} - \frac{3E_R}{2m_\chi v^2} \right]\end{aligned}$$

where $\mu_p = \frac{m_\chi m_p}{m_\chi + m_p}$ is the reduced mass of the DM-proton system. The last term in the above equation can be dropped for large values of DM mass. And so we get the following expression for the differential cross section per unit energy,

$$\frac{d\sigma}{dE_R} = \frac{e^2\mu^2}{4\pi E_R} \left[1 + \frac{E_R}{2\mu_p v^2} \right]. \quad (\text{A13})$$

Total Cross Section for Inelastic Scattering

In the case of inelastic scattering we consider the WIMPs as Majorana particles. As mentioned before in the main section that the differential scattering cross section in both elastic and inelastic scattering is the same. But the total cross sections in the two cases are related to each other as in eqn.(9). Now for inelastic scattering we have,

$$\begin{aligned}k_1^2 - k_2^2 &= 2\mu_N \delta \\ \text{or } k_2^2 &= k_1^2 - 2\mu_N \delta.\end{aligned}$$

The magnitude of the momentum transferred (working in CM frame) is then,

$$\begin{aligned}q^2 &= k_1^2 + k_2^2 - 2k_1 k_2 \cos \theta \\ &= 2k_1^2 \left(1 - \sqrt{1 - \frac{2\delta}{\mu_N v^2}} \cos \theta \right) - 2\mu_N \delta\end{aligned}$$

where we have used $k_1^2 = \mu_N^2 v^2$. And so,

$$dq^2 = -2k_1^2 \sqrt{1 - \frac{2\delta}{\mu_N v^2}} d(\cos \theta).$$

But $dq^2 = 2m_N dE_R$, therefore

$$dE_R = -\frac{k_1^2}{m_N} \sqrt{1 - \frac{2\delta}{\mu_N v^2}} d(\cos \theta).$$

The above equation in the elastic case becomes

$$dE_R = -\frac{k_1^2}{m_N}d(\cos \theta).$$

Now the total cross section for elastic scattering is given by,

$$\begin{aligned}\sigma_{elastic} &= \int \frac{d\sigma_{elastic}}{dE_R}dE_R \\ &= \frac{2\pi k_1^2}{m_N} \int \frac{d\sigma_{elastic}}{d\Omega}d(\cos \theta).\end{aligned}$$

For the inelastic case we have,

$$\begin{aligned}\sigma_{inelastic} &= \frac{2\pi k_1^2}{m_N} \sqrt{1 - \frac{2\delta}{\mu_N v^2}} \int \frac{d\sigma_{elastic}}{d\Omega}d(\cos \theta) \\ &= \sqrt{1 - \frac{2\delta}{\mu_N v^2}} \sigma_{elastic}.\end{aligned}$$

Appendix B: Annihilation Cross Section of Majorana DM

The process involved here is $\chi_1(k_1)\bar{\chi}_2(k_2) \rightarrow f(p_1)\bar{f}(p_2)$, f being a fermion of charge e with negligible mass. Now we work in the CM frame where,

$$\begin{aligned}k_1 &= (E_1, 0, 0, k), & k_2 &= (E_2, 0, 0, -k), \\ p_1 &= (E_f, E_f \sin \theta, 0, E_f \cos \theta), & p_2 &= (E_f, E_f \sin \theta, 0, E_f \cos \theta), \\ q &= p_1 + p_2, & q^2 &= 4E_f^2.\end{aligned}$$

The amplitude squared for this process is given by

$$|\mathcal{M}|^2 = \frac{e^2 g^2}{q^4} q^\alpha q^\beta [v(k_2)\bar{v}(k_2)\Gamma_{\mu\alpha}u(k_1)\bar{u}(k_1)\Gamma_{\nu\beta}][u(p_1)\bar{u}(p_1)\gamma^\mu v(p_2)\bar{v}(p_2)\gamma^\nu] \quad (\text{B1})$$

where $\Gamma_{\mu\alpha} = \sigma_{\mu\alpha}$ and $g = \mu$ for magnetic dipole interaction, whereas for electric dipole interaction $\Gamma_{\mu\alpha} = \sigma_{\mu\alpha}\gamma_5$ and $g = \mathcal{D}$. For Majorana particles,

$$\psi(x) = \sum_{s=1,2} \int \frac{d^3k}{(2\pi)^3 2k_0} [b_s(k)u_s(k)e^{-ikx} + b_s^\dagger v_s(k)e^{ikx}] \quad (\text{B2})$$

In the Majorana representation of γ -matrices, $C = -\gamma_0$ and the Majorana condition implies that $\psi = \psi^c = C\bar{\psi}^T = \psi^*$. Imposing $\psi = \psi^*$ on (B2) we get the relation $u_s = v_s^*$. Using this relation we can rewrite eqn.(B1) as

$$|\mathcal{M}|^2 = \frac{e^2 g^2}{q^4} q^\alpha q^\beta [v(k_2)u^T(k_2)\gamma_0\Gamma_{\mu\alpha}u(k_1)v^T(k_1)\gamma_0\Gamma_{\nu\beta}][u(p_1)\bar{u}(p_1)\gamma^\mu v(p_2)\bar{v}(p_2)\gamma^\nu]. \quad (\text{B3})$$

Now the spin sum rules for Majorana fermions are given by [16]

$$\sum_s u_s(p)v_s^T(p) = (\not{p} + m)C^T \quad (\text{B4})$$

$$\sum_s v_s(p)u_s^T(p) = (\not{p} - m)C^T \quad (\text{B5})$$

where $C^T = \gamma_0$. We then take the sum over spins of eqn.(B3) and use eqns.(B4) and (B5) to obtain

$$\overline{|\mathcal{M}|^2} = \frac{e^2 g^2}{4q^4} q^\alpha q^\beta \text{Tr}[(\not{k}_2 - m_2)\Gamma_{\mu\alpha}(\not{k}_1 + m_1)\Gamma_{\nu\beta}] \text{Tr}[\not{p}_1\gamma^\mu\not{p}_2\gamma^\nu] \quad (\text{B6})$$

where m_1 and m_2 are masses of χ_1 and χ_2 respectively. Now we discuss the two cases, beginning with the electric dipole case first.

Electric Dipole interaction

Eqn.(B6) with $g = \mathcal{D}$ and $\Gamma_{\mu\nu} = \sigma_{\mu\nu}\gamma_5$ yields the following expression for the averaged amplitude squared,

$$\overline{|\mathcal{M}|^2} = \frac{e^2 \mathcal{D}^2}{4q^4} (p_1 \cdot p_2) [(k_1 \cdot p_1)(k_1 \cdot p_2) + (k_2 \cdot p_1)(k_2 \cdot p_2) - (p_1 \cdot p_2)m_1 m_2] \quad (\text{B7})$$

where $q = p_1 + p_2$. Now in CM frame,

$$\begin{aligned} k_1 \cdot p_1 &= E_1 E_f - k E_f \cos \theta & k_1 \cdot p_2 &= E_1 E_f + k E_f \cos \theta \\ k_2 \cdot p_1 &= E_2 E_f + k E_f \cos \theta & k_2 \cdot p_2 &= E_2 E_f - k E_f \cos \theta \\ p_1 \cdot p_2 &= \frac{q^2}{2} & q^2 &= 4E_f^2 \end{aligned}$$

Using these in eqn.(B7) we get

$$\begin{aligned} \overline{|\mathcal{M}|^2} &= 4e^2 \mathcal{D}^2 [E_1 E_2 - k^2 \cos^2 \theta - m_1 m_2] \\ &= 4e^2 \mathcal{D}^2 E_1 E_2 \left[\left(1 - \frac{m_1 m_2}{E_1 E_2} \right) + \left(1 - \frac{(s - m_1^2 - m_2^2)}{2E_1 E_2} \right) \cos^2 \theta \right] \end{aligned} \quad (\text{B8})$$

where we use $k = \frac{s}{2} - E_1 E_2 - \frac{(m_1^2 + m_2^2)}{2}$ with $s = (E_1 + E_2)^2$.

The differential cross section in the CM frame is given by

$$\begin{aligned}\frac{d\sigma}{d\Omega} &= \frac{1}{64\pi^2 E_1 E_2 v_{rel}} \frac{E_f}{\sqrt{s}} \overline{|\mathcal{M}|^2} \\ &= \frac{e^2 \mathcal{D}^2}{32\pi^2 v_{rel}} \left[\left(1 - \frac{m_1 m_2}{E_1 E_2}\right) + \left(1 - \frac{(s - m_1^2 - m_2^2)}{2E_1 E_2}\right) \cos^2 \theta \right]\end{aligned}\quad (\text{B9})$$

where $E_f = \frac{\sqrt{s}}{2}$. Integrating above equation over $d\Omega$ gives the total cross section as

$$\sigma v_{rel} = \frac{e^2 \mathcal{D}^2}{8\pi} \left[\left(1 - \frac{m_1 m_2}{E_1 E_2}\right) + \frac{1}{3} \left(1 - \frac{(s - m_1^2 - m_2^2)}{2E_1 E_2}\right) \right]. \quad (\text{B10})$$

Eqn.(12) can be obtained by taking $m_1 = m_2$ and $E_1 = E_2$ in the above equation.

Magnetic Dipole Interaction

For the magnetic dipole case, with $g = \mu$ and $\Gamma_{\mu\nu} = \sigma_{\mu\nu}$ in eqn.(B6), the averaged amplitude squared reads

$$\overline{|\mathcal{M}|^2} = \frac{e^2 \mu^2}{4q^4} (p_1 \cdot p_2) [(k_1 \cdot p_1)(k_1 \cdot p_2) + (k_2 \cdot p_1)(k_2 \cdot p_2) + (p_1 \cdot p_2)m_1 m_2] \quad (\text{B11})$$

and this equation in the CM frame looks like

$$\overline{|\mathcal{M}|^2} = 4e^2 \mu^2 E_1 E_2 \left[\left(1 + \frac{m_1 m_2}{E_1 E_2}\right) + \left(1 - \frac{(s - m_1^2 - m_2^2)}{2E_1 E_2}\right) \cos^2 \theta \right]. \quad (\text{B12})$$

The total cross section is then given by

$$\sigma v_{rel} = \frac{e^2 \mu^2}{8\pi} \left[\left(1 + \frac{m_1 m_2}{E_1 E_2}\right) + \frac{1}{3} \left(1 - \frac{(s - m_1^2 - m_2^2)}{2E_1 E_2}\right) \right]. \quad (\text{B13})$$

One can obtain eqn.(13) by taking $m_1 = m_2$ and $E_1 = E_2$ in the above formula.

Appendix C: Event Rate for DM-Nucleus Elastic Scattering through Scalar Interaction

Here we consider scattering of DM and nucleus through scalar mediated spin-independent interaction. The details of this calculation are given in [2]. Here we shall give only the results of the calculation. The differential recoil rate per unit detector mass for DM-proton scattering can be written as

$$\frac{dR}{dE_R} = \frac{\rho_\chi \sigma_p A^2}{2m_\chi \mu_p^2} \int_{v > v_{min}} dv \frac{f(v)}{v} \quad (\text{C1})$$

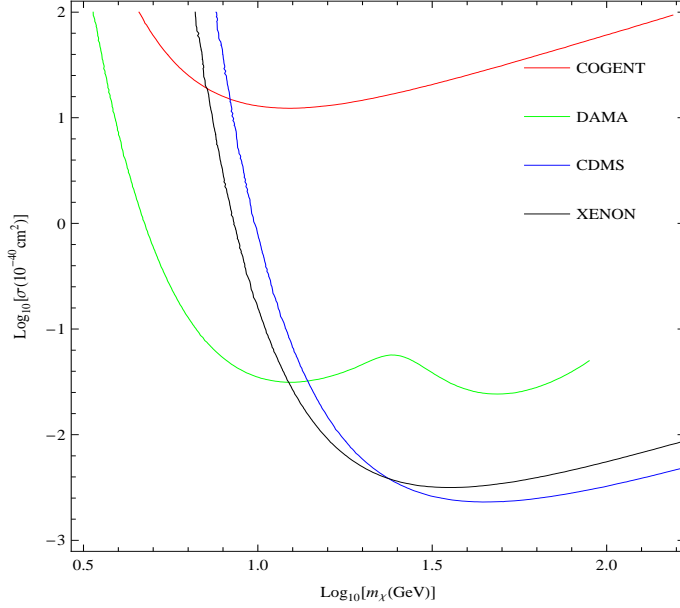


Figure 8: Plot shows variation of spin-independent DM-nucleus scattering cross section as a function of the DM mass for different experiments.

where $q = \sqrt{m_N E_R}$ is the nucleus recoil momentum, σ_p is the DM-proton cross-section, A is the number of nucleons and μ_p is the reduced mass of the DM-proton system. Here $F(E_R)$ is the Woods-Saxon form factor given by

$$F(E_R) = \frac{3j_1(qr)}{qr} e^{-q^2 s^2} \quad (\text{C2})$$

where $q = \sqrt{2m_N E_R}$ is the momentum transferred, m_N being the nucleus mass, $s \simeq 1$ fm and $r = \sqrt{R^2 - 5s^2}$ with $R = 1.2A^{1/3}$ fm. The spin-independent differential cross section for contact interaction scattering is given by

$$\frac{d\sigma}{d|\mathbf{q}|^2} = G_F^2 \frac{C}{v^2} F^2(E_R) = \frac{\sigma_0}{4\mu_N^2 v^2} F^2(E_R) \quad (\text{C3})$$

where

$$C = \frac{1}{\pi G_F^2} [Z f_p + (A - Z) f_n]^2 \quad (\text{C4})$$

$$\sigma_0 = \int_0^{4\mu_N^2 v^2} \frac{d\sigma(q=0)}{d|\mathbf{q}|^2} d|\mathbf{q}|^2 = \frac{4\mu_N^2}{\pi} [Z f_p + (A - Z) f_n]^2 \quad (\text{C5})$$

Here $|\mathbf{q}|^2 = 2m_N E_R$ is the magnitude square of the momentum transferred, μ_N is the reduced mass of the DM-nucleus system, Z is the number of protons and A is the number

of nucleons. Taking $f_p \sim f_n$ we can write the DM-nucleus cross section in terms of the DM-proton cross section[7] using eqn.(C5) as

$$\sigma_0 = \frac{\mu_N^2}{\mu_p^2} A^2 \sigma_p \quad (\text{C6})$$

where μ_p is the reduced mass of the proton-DM system. Substituting from eqn.(C6) in eqn.(C3) we have

$$\frac{d\sigma}{d|\mathbf{q}|^2} = \frac{\sigma_p A^2}{4\mu_p^2 v^2} F^2(E_R) \quad (\text{C7})$$

The differential rate per unit detector mass can be written as

$$dR = \frac{\rho_\chi}{m_\chi m_N} \left(\frac{d\sigma}{d|\mathbf{q}|^2} \right) f(v) v dv d|\mathbf{q}|^2 \quad (\text{C8})$$

where the quantity f is as defined in the main section. Substituting from eqn.(C7) in the above equation we get

$$dR = \frac{\rho_\chi \sigma_p A^2}{4m_\chi m_N \mu_p^2} F^2(E_R) \left(\frac{f(v)}{v} \right) dv d|\mathbf{q}|^2 \quad (\text{C9})$$

Using $d|\mathbf{q}|^2 = 2m_N dE_R$ we get the differential rate per unit recoil energy,

$$\frac{dR}{dE_R} = \frac{\rho_\chi \sigma_p A^2}{2m_\chi \mu_p^2} F^2(E_R) \int_{v>v_{min}} \frac{f(v)}{v} dv$$

which is same as eqn.(C1).

References

- [1] M. Drees and G. Gerbier in PDG compilation, C. Amsler et al., Physics Letters **B667**, 1 (2008).
- [2] G. Jungman, M. Kamionkowski and K. Griest, Phys. Rep. **267**, 195 (1996).
- [3] J. Angle *et al.* [XENON10 Collaboration], Phys. Rev. Lett. **101**, 091301 (2008) [arXiv:astro-ph/0802.3530].
- [4] Z. Ahmed *et al.* [CDMS Collaboration], Phys.Rev. Lett. **102**, 011301 (2009) [arXiv:astro-ph/0802.3530].
- [5] R. Bernabei *et al.* [DAMA Collaboration], arXiv:0804.2741 [astro-ph].

- [6] C. Aalseth *et al.* [CoGeNT Collaboration], Phys. Rev. Lett. **101**, 251301 (2008) [arXiv:astro-ph/0807.0879].
- [7] C. Savage, G. Gelmini, P. Gondolo and K. Freese, arXiv:0808.3607 [astro-ph].
- [8] A. Bottino, F. Donato, N. Fornengo and S. Scopel, Phys. Rev. D **78**, 083520 (2008) [arXiv:hep-ph/0806.4099].
- [9] D. Tucker-Smith and N. Weiner, Phys. Rev. D **64**, 043502 (2001) [arXiv:hep-ph/0101138]; D. Tucker-Smith and N. Weiner, Phys. Rev. D **72**, 063509 (2005) [arXiv:hep-ph/0402065]; S. Chang, G. D. Kribs, D. Tucker-Smith and N. Weiner, arXiv:0807.2250 [hep-ph].
- [10] M. Pospelov and T. Veldhuis, Phys. Lett. **B 480**, 181 (2000) [arXiv:hep-ph/0003010].
- [11] K. Sigurdson, M. Doran, A. Kurylov, R. R. Caldwell and M. Kamionkowski, Phys. Rev. D **70**, 083501 (2004) [Erratum-ibid. D **73**, 089903 (2006)] [arXiv:astro-ph/0406355].
- [12] M. Acciarri *et al.* [L3 Collaboration], e- Phys. Lett. B **412**, 201 (1997).
- [13] E. Komatsu *et al.* [WMAP Collaboration], Astrophys. J. Suppl. **180**, 330 (2009) [arXiv:0803.0547 [astro-ph]].
- [14] V. Barger, W. Y. Keung and G. Shaughnessy, Phys. Rev. D **78**, 056007 (2008) [arXiv:0806.1962 [hep-ph]].
- [15] E. W. Kolb and M. S. Turner, Front. Phys. **69**, 1 (1990).
- [16] H. E. Haber and G. L. Kane, Phys. Rept. **117**, 75 (1985).